Effect of Mechanical Properties Using Different Filler Metals on Wide-Clearance Activated-Diffusion-Brazed Ni-Based Superalloy

C.Y. Su, C.P. Chou, W.J. Chang, and M.H. Liu

(Submitted 30 March 1999; in revised form 11 June 1999)

The investigation of mechanical properties and failure mechanism of activated-diffusion-brazed (ADB) joints in IN-738 plate were conducted. Joints of this type, which had wide clearance, were formed using the brazing alloys Nicrobraz 150 and DF4B. The microstructural characterization showed that chromium borides with a blocky morphology were present in joints associated with the two brazing alloys. A major difference in matrix phase chemistry was observed, however, for the two brazing alloys, *e.g.*, an Ni-B eutectic phase was observed in Nicrobraz 150, but DF4B exhibited a coarsened gamma prime (γ) phase and an absence of a nickel boride matrix phase. Results of tensile test showed that ADB specimens using DF4B brazing alloy exhibited 95% nominal tensile strength of IN-738 base materials. Fracture cracks in the joint area were initiated and confined to dispersed chromium boride sites. However, tensile test of ADB specimens using Nicrobraz 150 showed poor tensile properties at all testing temperatures, and their fractures were initiated at a brittle nickel boride site and propagated along the weak-bonded interface between the Ni-B eutectic phase and base materials.

Keywords activated diffusion brazed, additive metal, filler metal, isothermal solidification, transient liquid phase sintering

1. Introduction

The wide clearance of activated-diffusion-brazed (ADB) joints with nickel-based filler metals is widely used for repairing and joining of land-based and aero engine components.[1–5] To obtain wide clearance, the use of a third component (additive metal) besides the filler metal and the base metal becomes necessary. The reaction of the additive metal powders and filler metal powders will strongly affect the mechanical properties of the joint area during the ADB process. The bonding mechanism of ADB joints is similar to the mechanism of the transient liquid phase sintering technique in which filler metal becomes liquid on heating process. Figure 1 illustrates the schematic diagram of different stages in the brazed zone of the ADB joint. At stage 1, eutectic liquid forms in the filler metal. At stage 2, the rearrangement stage, eutectic liquid of filler metal begins to spread on the surface of additive metal and diffuses into the base metals; at the same time, the base metal is partially melted by the eutectic liquid. At stage 3, grain growth, pore elimination, and contact growth result in a microstructure of grains surrounded by the solidified liquid phase. The melting point depressants form hard and brittle intermetallic compounds with the elements of base metal and those compounds will determine the mechanical properties of the brazed joints.

C.Y. Su, W.J. Chang, and **M.H. Liu,** Industrial Technology Research Institute, Materials Research Laboratories, Hsinchu, Taiwan, Republic of China; and **C.P. Chou,** Department of Mechanical Engineering, National Chiao Tung University, Hsinchu, Taiwan, Republic of China. Contact e-mail: CherngYuhSu@itri.org.tw.

Numerous studies[6–10] in the wide-clearance joint have documented the brazing microstructures in simple alloy systems. Those publications focus on microstructural characterizations of joined specimens using binary or ternary alloys as filler metal and additive metal. Because of the complexity of processing superalloy powders *via* ADB techniques, little is known about the effects of the chemical composition of filler metal on the final properties of the completed ADB process. Binary or even ternary phase diagrams can provide only limited information about the microstructural development in these alloys. Most of the data available in the literature have been obtained by experimental observations. In this study, the microstructure and its effects on fracture mechanism in the tensile tested specimen of joined IN-738 with Ni-Cr-B-based filler metals will be discussed.

2. Experimental Procedure

The base metal and the additive material used in this study are IN-738 nickel-based superalloy. The IN-738 substrate was prepared as a 60 × 60 × 3 mm (L × W × H) coupon with 1 mm root gap for a V type joint. Filler metals are inert gas-atomized Nicrobraz 150 and DF4B powders. Nominal compositions of these selected materials are listed in Table 1. Prior to the ADB process, the faying surface of IN-738 base metal was electroplated with a nickel layer of 0.03 mm thickness. Brazed powder mixtures were prepared by mixing filler metal and additive materials powder with different weight percentages, 30/70, 40/60, and 50/50. The weighted powders were put into small cylindrical plastic capsules and mixed thoroughly in a three-dimensional mixer for 2 h. The brazed process was conducted in a vacuum furnace under 4×10^{-5} torr (5×10^{-3} Pa). A typical thermal cycle of the ADB process used in this study is shown in Fig. 2.

Table 1 Nominal compositions of IN-738 (base materials and additive metal) and braze alloys

Element (wt.%)	Cr	Co	Al	Ti	W	Mo	Ta	Nb	B	C	Zr	Y	Ni
IN-738	16.0	8.4	3.4	3.4	2.7	1.7	1.7	0.8	0.01	0.1	0.03	⋯	Bal
Nicrobraz 150	15.0	⋯	⋯	⋯	⋯	⋯	⋯	⋯	3.5	0.1	⋯	⋯	Bal
DF4B	14.0	10.0	3.5	⋯	⋯	⋯	2.5	⋯	2.7	⋯	⋯	0.02	Bal

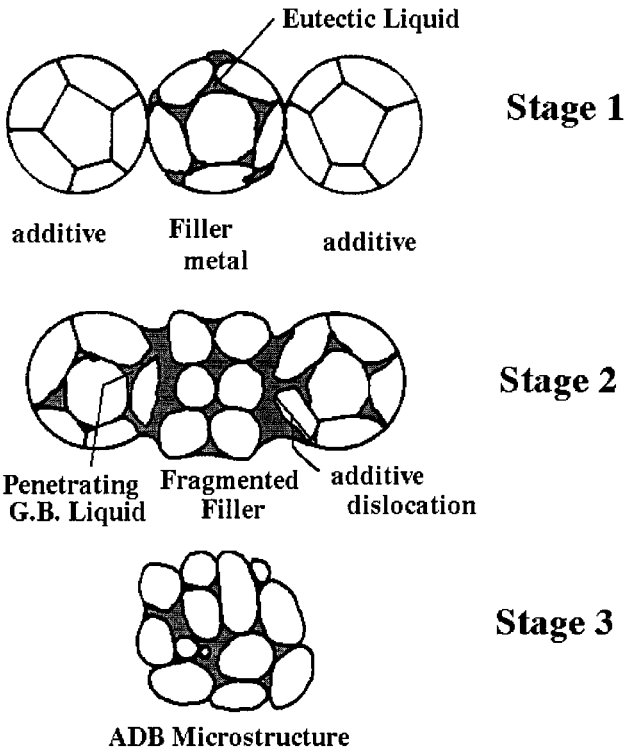

Fig. 1 The schematic diagram illustrates the different stages in the brazed zone of the ADB process

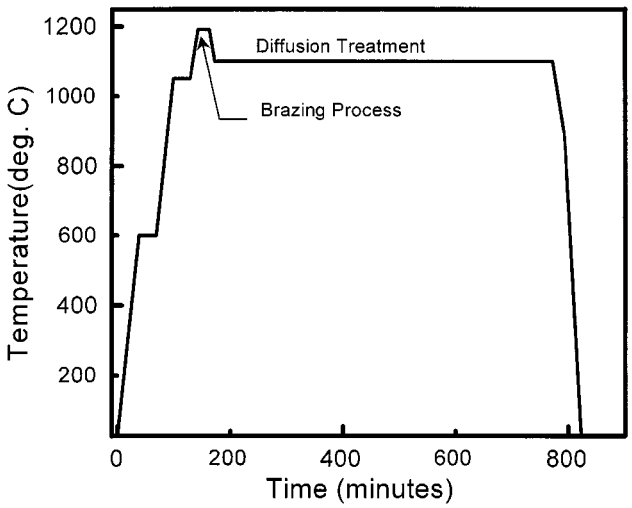

Fig. 2 Schematic illustration of the thermal cycle used in this investigation

Tensile test specimens were machined from joint samples according to ASTM E8M. Tensile tests were performed with strain rate of 0.0125/s at room temperature, 760 °C, and 980 °C. Microstructural observations were made on a cross-sectional sample using optical microscope, scanning electron microscope, and electron probe x-ray microanalyzer (EPMA). The EPMA analysis was conducted using a JEOL JXA-8800M microscope (Japan Electron Optics Ltd., Tokyo) operated at an accelerating voltage of 15 V, and a specimen current of 1×10^{-7} A was used for detecting boron and carbon.

3. Results and Discussion

3.1 Microstructure Examination

Figure 3(a) and (b) present the microstructure of the IN-738 specimen joined by 40 wt.% Nicrobraz 150 filler metal plus 60 wt.% additive metal. Two intermetallic compounds can be observed in the brazed area. Table 2 shows the chemical compositions for the two phases. The results of quantitative analysis indicates that the phase marked **a** is based on Cr (B,C). The phase marked **b** is predominantly as Ni_3B, and the phase marked **c** is the γ phase of nickel solid solution.

A previous study[11] about the wettability of Nicrobraz 150 and DF4B on the IN738 surface showed that the spreading index of Nicrobraz 150 is two times higher than that of DF4B, and it is related to a relatively lower rate of isothermal solidification. Figure 3(a) shows that Nicrobraz 150 spreads sufficiently on the surface of additive metal in the rearrangement stage. Grain growth, shape accommodation, contact growth, and pore elimination occurred in stages afterward. However, the results of quantitative analysis indicated that chemical homogenization occurred in the mixed powder of additive metal and filler metal during ADB processing, where the difference in chemical potential of these two metals was the source of the driving force. From the result of chemical analysis, it was found that Ti, Mo, W, and Ta but not Al atoms diffused into Nicrobraz 150 from the additive metals; at the same time, B atoms diffused from filler metal into additive metals. It was reported[12] that the microstructure of solidified Nicrobraz 150 contains nickel boride, γ phase, and chromium boride after a conventional brazed joint process. After ADB processing, the liquefied Ni-B eutectic phase surrounded on the surface of additive-metal powders at the end of the ADB process, although much of the composite elements of additive metal are diffused to the site of Nicrobraz 150.

The microstructure of the joint specimen that used DF4B as filler metal showed that a strong chemical interaction occurred during the ADB process. However, it was found that there were only low concentrations on intermetallic compounds in the brazed zone. Figure 4 is a typical microstructure of the joint

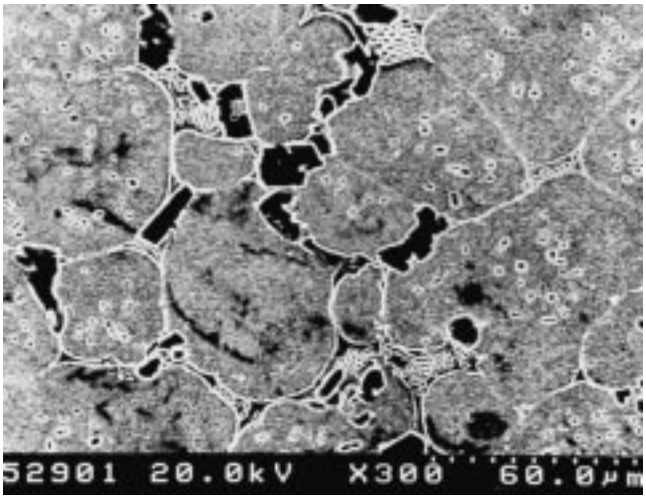

(a)

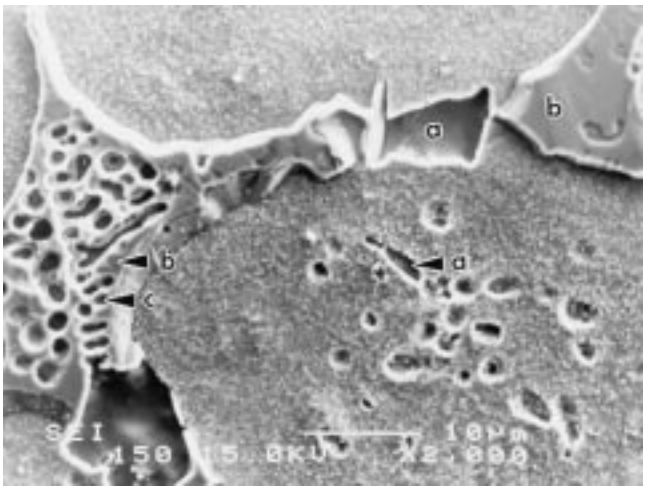

(b)

Fig. 3 The cross-sectional microstructure of 40 wt.% Nicrobraz 150 plus 60 wt.% additive metal after the ADB process. (**a**) Low magnification, 300×; and (**b**) high magnification, 2000×

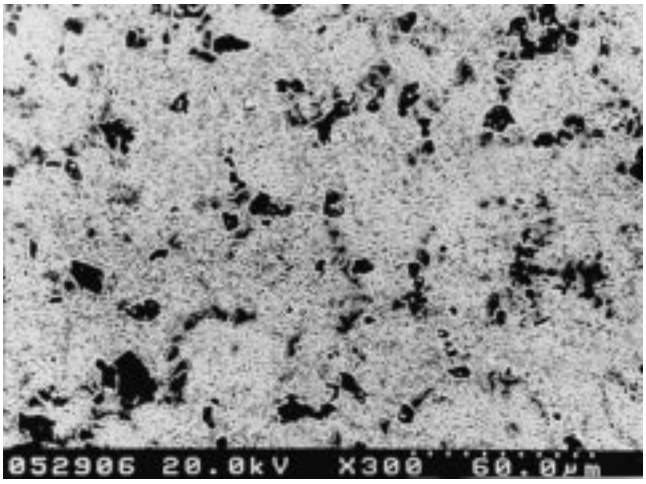

(a)

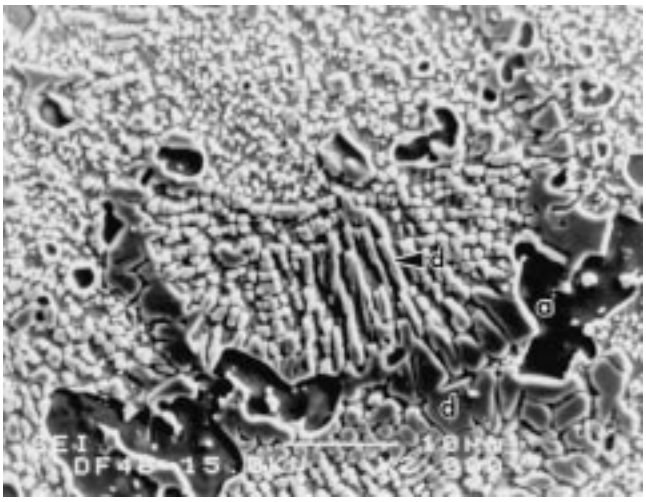

(b)

Fig. 4 Microstructures of the brazed joint produced by mixed 40 wt.% Nicrobraz 150. (**a**) Low magnification, 300×; and (**b**) high magnification, 2000×

Table 2 Composition analysis of phases in sample of 40 wt.% of Nicrobraz 150 filler metal

Element		Ni	Cr	Co	Al	Ti	W	Mo	Ta	Nb	B	C	Identification of intermetallic
a phase	Wt.%	4.8	68.9	1.9	0.0	0.3	4.5	6.0	0.0	0.0	7.1	6.5	Cr (B,C)
	At.%	3.0	48.4	1.1	0.0	0.2	0.9	2.3	0.0	0.0	24.1	20.0	
b phase	Wt.%	76.2	4.8	5.8	0.6	5.1	0.4	0.3	2.3	1.4	1.4	1.7	Ni_3B
	At.%	67.5	4.8	5.1	1.1	5.5	0.1	0.1	0.7	0.8	7.0	7.3	

specimen after ADB processing with 40 wt.% DF4B filler metal plus 60 wt.% IN-738 additive metal. The results of compositional analyses are shown in Table 3. Note that the Cr (B,C) is still present. However, the matrix Ni_3B as for Nicrobraz 150 (shown in Fig. 3b) was not clearly observed. The stoichiometry of the irregular blocklike darker phase along the Cr (B,C) phase was analyzed to be a γ' phase; the phase marked **d** is indicated in Fig. 4(b). The γ' phase is the major strengthening phase of IN-738 and was precipitated in the filler metal site instead of in the Ni-B eutectic phase.

The bonding behavior of the ADB process using DF4B filler metal can be summarized as follows. At first, Ni-B eutectic liquid of DF4B occurred along grain boundaries and began to alloy with solid-state additive materials. Therefore, no cluster

Table 3 Composition analysis of phases in sample of 40 wt.% of DF4B filler metal

Element		Ni	Cr	Co	Al	Ti	W	Mo	Ta	Nb	B	C	Identification of intermetallic
a phase	Wt.%	4.7	70.2	3.7	0.0	0.5	5.8	5.8	0.7	0.1	6.1	2.4	Cr (B,C)
	At.%	3.3	57.2	2.7	0.0	0.5	1.3	2.6	0.2	0.1	23.8	8.3	
b phase	Wt.%	73.3	3.5	6.1	6.9	4.5	0.3	0.3	3.9	0.5	0.0	0.7	Ni_3B
	At.%	67.3	3.6	5.5	13.7	5.1	0.1	0.1	1.2	0.3	0.0	3.1	

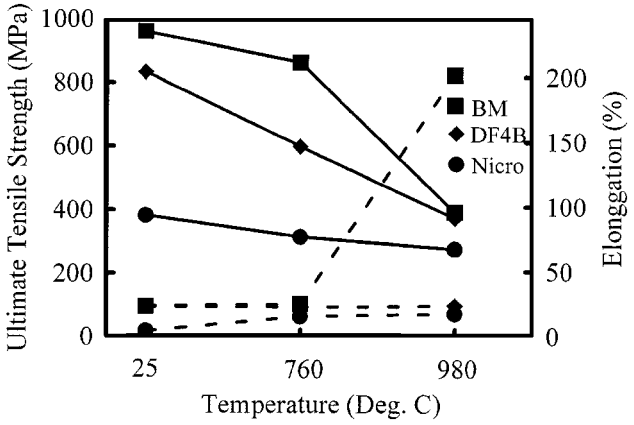

Fig. 5 Mechanical properties of ADB joints and base materials. In this figure, the solid line illustrates the ultimate strength values (MPa) and the dashed line illustrates the elongation values (%). BM is base metal

of Ni-B eutectic liquid was formed at the grain boundary. After the post-ADB heat treatment, the γ' phase was precipitated in the Ni-B eutectic liquid. Since Cr (B,C) is a morphologically stable phase at all temperatures within the diffusion process, its chemical composition does not change once it has been nucleated.[13] Compared with the microstructure of joint specimens with Nicrobraz 150 filler metal, Al plays an important role during the diffusion process with DF4B filler metal. Lugscheider[14] reported that the species in the surface layer of Ni-based superalloy after 1150 °C heat treating in a vacuum 2×10^{-3} Pa still contain aluminum oxide (Al_2O_3) and Ti, the elements of base metal. This implies that, even in a high vacuum environment, Al is still active to interact with oxygen and carbon.

3.2 Mechanical Properties

Based on the microstructural analysis of specimens joined by 30 wt.% DF4B filler metal, there existed many pores in the entire brazed zone. In the specimen joined by 50 wt.% DF4B filler metal, many hard-brittle intermetallic phases of Cr (B,C) appeared. Therefore, the specimens joined by 40 wt.% filler metals, Nicrobraz 150 and DF4B, plus 60 wt.% additive metal were selected for tensile testing, and designated as "Nicro" and "DF4B" specimen, respectively, and "BM" represents the specimen of IN-738 base metal.

Figure 5 shows the result of tensile tests. All of the tested specimens were broken at the joint region after testing. The ultimate tensile strength (UTS) of the DF4B specimen at 980 °C is nearly identical to that of the base metal specimen, 372.4 MPa versus 392 MPa, and its UTS at room temperature achieves 85% of that of the base metal specimen. However, Nicrobraz 150 specimens showed poor tensile properties at all testing temperatures.

(a)

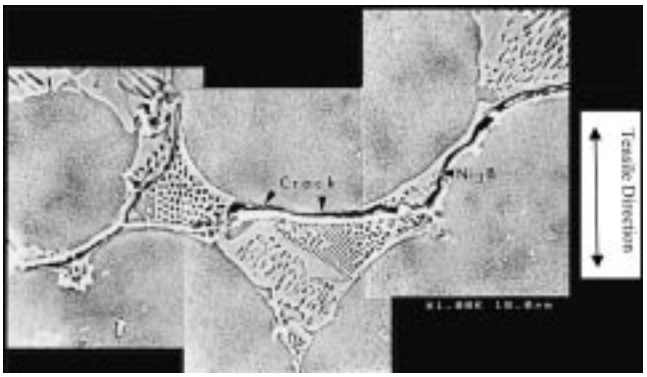

(b)

Fig. 6 (**a**) Fracture surface of Nicrobraz 150 specimen at room temperature; and (**b**) microstructure of deformed Nicrobraz 150 specimen at room temperature

Figure 6(a) is the fractograph of the Nicro specimen tested at room temperature. It reveals the brittle fracture characteristic of IN-738 after ADB joining by Nicrobraz 150 filler metal. From the side view of the fracture surface as shown in Fig. 6(b), the source of crack was initiated at the Ni_3B phase and propagated along the interface of Ni_3B and additive metal. This

(a)

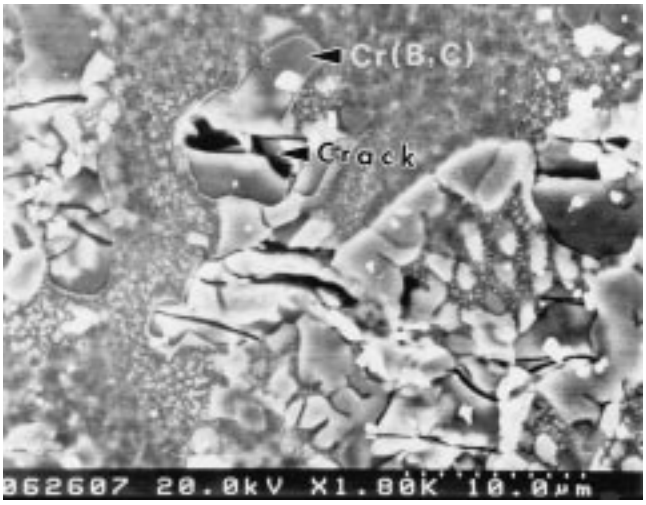

(b)

Fig. 7 (**a**) Fracture surface of DF4B specimen at room temperature; and (**b**) microstructure of deformed DF4B specimen at room temperature

might have resulted from the hard and brittle characteristic of the Ni_3B phase and poor alloyed reaction between Nicrobraz 150 and additive metal powders.

Figure 7(a) is the fractograph of the DF4B specimen tested at room temperature. As shown in this figure, the fracture surface contained both brittle and ductile modes. Cracks were initiated at pore and Cr (B,C) sites due to the brittle nature of the Cr (B,C) phase (Fig. 7b). Since the joined DF4B specimen is nearly pore free (Fig. 4), the UTS of the DF4B specimen can reach 95% UTS of the base metal even at 980 °C. However, the existence of the brittle Cr (B,C) phase results in poor elongation of joined specimens.

The fracture path in the brazed zone of the wide-clearance ADB process is schematically illustrated in Fig. 8. As shown in Fig. 8(a), fracture of the Nicrobraz specimen was initiated at the N′3B phase. Since the major bonding in the brazed zone of the Nicrobraz 150 specimen is from the chain-type structure

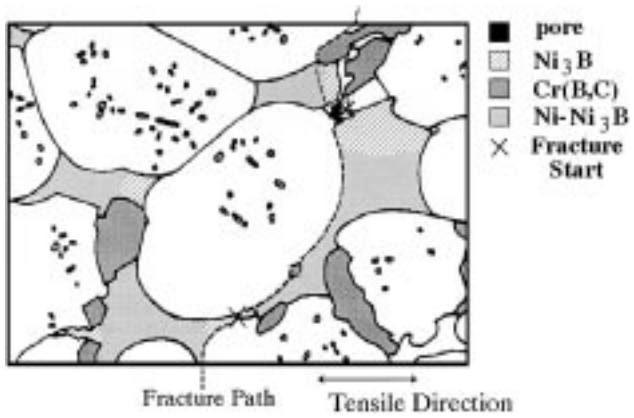

(a)

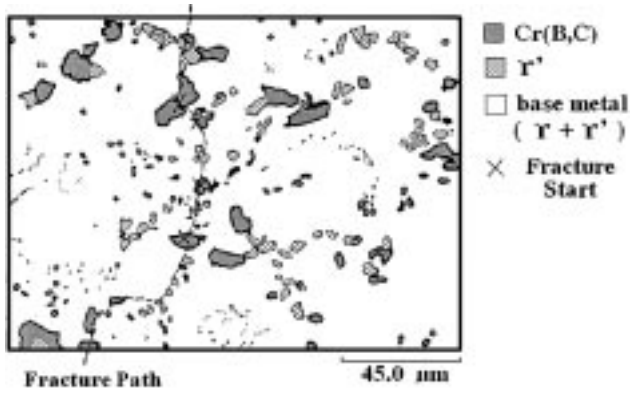

(b)

Fig. 8 Fractured path of the brazed zone of wide-clearance ADB sample with different brazing alloys. (**a**) Nicrobraz 150 and (**b**) DF4B

formed by additive metal powders surrounded by solidified Ni-B eutectic (Fig. 3), the bonding interaction at the interface between additive metal powders and Ni-B eutectic is weak. Therefore, cracks propagated along this weak-bonded interface, whereas in the brazed zone of the DF4B specimen, cracks were initiated at dispersed Cr (B,C) sites and passed through the more ductile γ phase and the γ' phase (Fig. 8b and Fig. 4).

4. Conclusions

Nicrobraz 150 filler metal showed excellent wettability on the surface of IN-738 additive metal. However, lack of alloying reaction between filler metal and additive metal resulted in the reduction of the interface strength. In contrast, the precipitation of the γ' phase on the site of DF4B filler metal can strengthen the brazed zone of wide-clearance ADB joined specimens. The joined DF4B specimens showed 85% UTS of IN-738 base metal at room temperature and 95% UTS of IN-738 base metal at 980 °C.

Fractures were initiated at brittle Ni_3B sites and propagated along the weak-bonded interface between Ni-B eutectic and additive metal in the joined Nicro specimens and showed brittle fracture characteristics. Cracks in the brazed zone of joined DF4B specimens were initiated and contained in dispersed

brittle Cr (B,C) sites. The specimens joined by DF4B filler metal showed brittle and ductile dual fracture characteristics.

References

1. P.R. Mobley and G.S. Hoppin III: *Weld. J.*, 1961, vol. 40 (6), pp. 610-17.
2. J.W. Lee, J.H. McMurray, and J.A. Miller: *Weld. J.*, 1985, vol. 64 (10), pp. 18-21.
3. D.S. Duvall, W.A. Owczarski, and D.F. Paulonis: *Weld. J.*, 1974, vol. 53 (4), pp. 203-14.
4. B.L. Gruzdev: *Weld. Int.*, 1988, No. 6, pp. 543-45.
5. F.J. Hermanek and M.J. Stern: *Turbine Component Restoration by Activated Diffusion Brazing*, Sulzer Plasma Technik, Inc., Switzerland, 1984.
6. E. Lugscheider, V. Dietrich, and J. Mittendorff: *Weld. J.*, 1988, vol. 67 (2), pp. 47-51.
7. J.W. Chasteen and G.E. Metzger: *Weld. J.*, 1979, vol. 58 (4), pp. 111-17.
8. E. Lugscheider, T. Schittny, and E. Halmoy: *Weld. J.*, 1989, vol. 68 (1), pp. 9-13.
9. S.K. Tung and L.C. Lim: *Mater. Sci. Technol.*, 1994, vol. 10 (5), pp. 364-69.
10. B. Jahnake and J. Demny: *Thin Solid Films*, 1983, vol. 110, pp. 225-35.
11. C.Y. Su, C.P. Chou, B.C. Wu, and W.C. Lih: *Mater. Sci. Technol.*, 1999, vol. 15 (3), pp. 316-22.
12. S.K. Tung and L.C. Lim: *Scripta Mater.*, 1996, vol. 34 (5), pp. 763-69.
13. R.G. Iacocca: *Metall. Mater. Trans. A*, 1996, vol. 27A, pp. 145-53.
14. E. Lugscheider, H. Zhuang, and M. Maier: *Weld. J.*, 1983, vol. 62 (10), pp. 295-300.